Two-state switching and dynamics in quantum dot two-section lasers

Two-state switching and dynamics in quantum dot two-section lasers

A. Markus,[a] M. Rossetti,[b] V. Calligari, D. Chek-Al-Kar, J. X. Chen,[c] and A. Fiore
Institute of Quantum Electronics and Photonics, Ecole Polytechnique Fédérale de Lausanne, Station 3, CH-1015 Lausanne, Switzerland

R. Scollo
Electronics Laboratory (IfE), Swiss Federal Institute of Technology (ETH), Zürich Gloriastrasse 35, CH-8092 Zürich, Switzerland

(Received 24 August 2006; accepted 7 September 2006; published online 5 December 2006)

The electrical control of the lasing wavelength in two-section quantum dot lasers is investigated. By changing the optical loss in the absorber section, the control of the ground-state (GS) and excited-state (ES) lasing thresholds and output powers is achieved. Additionally, a complex self-pulsation dynamics with simultaneous oscillations of the GS and ES intensities is observed. The experimental results are well explained in the framework of a rate equation model. © *2006 American Institute of Physics*. [DOI: 10.1063/1.2397293]

I. INTRODUCTION

Devices based on semiconductor quantum dots (QDs) offer potential advantages as compared to their quantum well (QW) counterparts. QD lasers with an emission wavelength around and well beyond 1.3 μm,[1–3] low threshold current,[2] low chirp,[4] and reduced temperature sensitivity[3,5] have been demonstrated. Lasing can be achieved on any of the QD discrete energy states, thus at well separated wavelengths, depending on the cavity loss. The corresponding interlevel carrier dynamics also leads to peculiar features such as simultaneous two-state lasing,[6,7] large gain compression,[8] and negative differential gain.[9,10] The possibility of varying the lasing wavelength in a broad range may be of interest, particularly if switching between the two fiber-transmission windows (1.3 and 1.55 μm) could be achieved. Preliminary evidence of wavelength switching was shown in Ref. 11, although in that case the two wavelengths were closely spaced ($\sim$16 nm), likely corresponding to the same QD energy state. In this paper we demonstrate the control of lasing threshold and output power of two well-separated lines at 1.28 and 1.19 μm, corresponding to the QD ground state (GS) and first excited state (ES), by varying the current in the absorber section of a two-section laser. Moreover, we experimentally and theoretically analyze the self-pulsation dynamics of two-state lasers, and evidence a unique regime of simultaneous GS and ES oscillations, which highlights the role of interlevel carrier relaxation.

II. RESULTS AND CALCULATIONS

The devices used in our experiments were fabricated from the same wafer described in Ref. 7 in detail. The epitaxial structure consists of an $Al_{0.7}Ga_{0.3}As/GaAs/Al_{0.7}Ga_{0.3}As$ waveguide with three layers of self-assembled InAs QDs, which are covered by a 5 nm $In_{0.15}Ga_{0.85}As$ QW and separated from each other by a 40 nm GaAs spacer layer. Ridge-waveguide (ridge width=4 μm) edge-emitting lasers have been fabricated from this structure with as cleaved facets, as already reported.[6,7] These devices operate on the GS transition at 1.28 μm for a cavity length $l > 2.5$ mm and on the ES transition at 1.22 μm for a cavity length $l < 1.5$ mm. For an intermediate cavity length of 1.5 mm $< l <$ 2.5 mm lasing takes place on both GS and ES transitions due to a combination of GS gain saturation and a slow intraband relaxation time.[6,7] The two-section lasers discussed in this letter have a 30 μm long and 0.15 μm deep etched gap in the ridge, which separates the *p*-type contact into two sections. The resistance between the two contacts was measured to be about 10 kΩ.

We first investigated the emission spectra from the facets of a two-section laser with a 2 mm long gain section and a 0.6 mm long absorber section at room temperature and in pulsed mode (1 μs pulses, 1% duty cycle to minimize heating effects). The device was measured with constant current injection in the gain section (J_g=1240 A/cm^2) and increasing current injection in the absorber section (270 A/cm^2 $< J_a <$ 1200 A/cm^2). The evolution of emission spectra detected from the facet of the absorber section with increasing absorber bias is shown in Fig. 1. At low absorber bias (J_a =270 A/cm^2), the total loss introduced by the absorber section into the cavity is too large to sustain lasing and only light stemming from spontaneous emission (SE) is detected with a peak value at 0.97 eV, corresponding to the GS transition. At an injection current of J_a=420 A/cm^2 on the absorber section the device starts lasing on the GS transition at 0.96 eV. With increasing absorber bias, the GS lasing line broadens and at J_a=910 A/cm^2 a second lasing line appears at the ES transition at 1.025 eV.

The quantitative behavior of GS/ES lasing thresholds is studied in Figs. 2(a) and 2(b), where the integrated intensities of GS and ES lines are shown, respectively, as a function of the current in the gain section, for different bias in the absorber section. GS and ES emissions have been detected

[a]Present address: Lichti + Partner GbR, Postfach 41 07 60, 76207 Karlsruhe, Germany.
[b]Electronic mail: marco.rossetti@epfl.ch
[c]Present address: Bell Laboratories, Lucent Technologies Inc., 600 Mountain Ave., Murray Hill, New Jersey 07974.

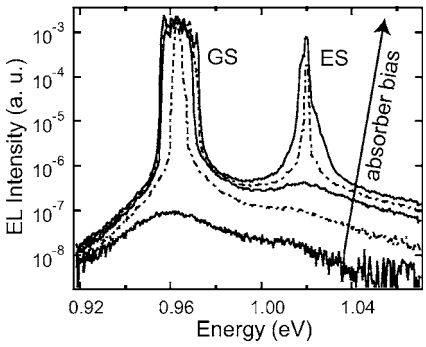

FIG. 1. Room temperature emission spectra of a QD two-section laser with a 2 mm long gain section and a 0.6 mm long absorber section detected from the facet of the absorber section at constant bias on the gain section (J_g = 1240 A/cm^2) and increasing bias on the absorber section (J_a = 270–1200 A/cm^2).

separately with high/low bandpass filters with a cut-on/off wavelength at 1250 nm. At low absorber bias, the optical loss in the absorber is too large to allow GS lasing, so that lasing is observed first in the ES transition at large gain current. Note, however, that as soon as ES turns on, the ES photons produce an ES population in the absorber, which relaxes down to the GS reducing the GS loss and threshold gain, so that GS lasing also turns on at the ES threshold. As absorber bias is increased, lasing occurs first on the GS, with a second ES threshold at larger currents, as observed in single-section lasers.[6] GS and ES threshold currents both decrease and differential efficiencies increase with increasing absorber bias, corresponding to lower optical loss/increasing gain in the absorber. Note that the mechanism of GS absorber bleaching under ES lasing conditions prevents the observation of a single ES lasing line. ES-only output is observed with a negative bias on the absorber, since photogenerated ES carriers in the absorber are, in this case, swept away by the field and cannot relax down to the GS. The inset of Fig. 2(b) displays two emission spectra, in which the complete switching from GS lasing (full line) to ES lasing (dashed line) has been achieved by changing the absorber voltage from V_a=0.1 V to V_a=−5.0 V and the laser bias from J_g=1080 A/cm^2 to J_g=1930 A/cm^2, thus demonstrating the functionality of wavelength switching between 1.28 and 1.19 μm.

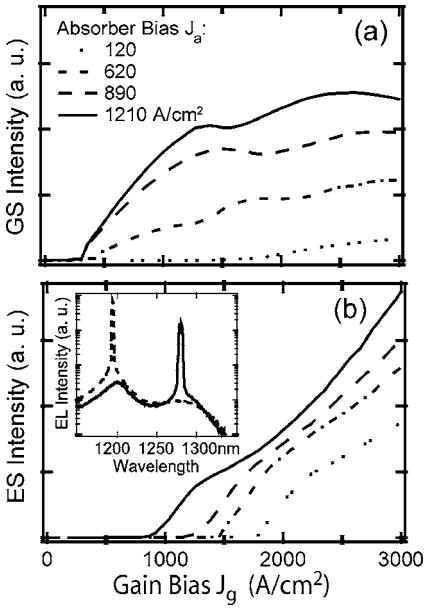

FIG. 2. Room-temperature, spectrally resolved GS (a) and ES (b) light-current characteristics from a QD two-section laser with a 2 mm long gain section and a 0.6 mm long absorber section at different current densities on the absorber section J_a. The inset of (b) displays two emission spectra, in which complete switching from GS lasing (full line: V_a=0.1 V, J_g = 1080 A/cm^2) to ES lasing (dashed line: V_a=5.0 V, J_g=1930 A/cm^2) has been achieved.

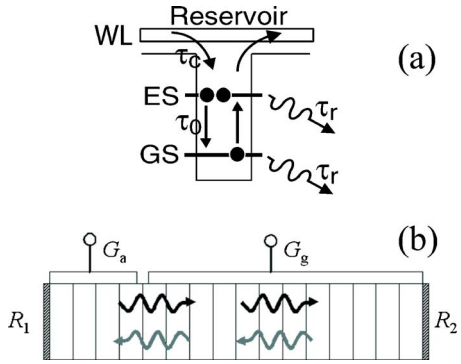

FIG. 3. Schematic of the traveling-wave rate equation model. (a) Structure of the dot energy levels describing the carrier dynamics. (b) Two-section optical cavity with forward- and backward-traveling photons.

In order to validate this interpretation of the complex behavior of GS/ES lasing thresholds, a traveling-wave rate equation model has been employed, similar to the one we proposed in Ref. 12 where differential equations for carriers injected into a reservoir energy level (WL) are coupled to the equations for the population of the ES and GS energy levels through capture from the WL to the ES (time constant τ_c), relaxation from the ES to the GS (time constant τ_0), thermal escape from the GS to the ES (time constant τ_{esc}^{GS}), and from the ES to the WL (time constant τ_{esc}^{ES}). A spatial dependence was also introduced in the equations describing the GS and ES photon numbers, which are divided into forward-traveling ($N_{\varphi+}$) and backward-traveling ($N_{\varphi-}$) photons and are amplified or absorbed along the cavity, depending on the injection regime. To reproduce the experimental data, it was indeed crucial to consider the spatial dependence of the field and gain inside the cavity due to the highly nonuniform geometry of a two-section device. It has been checked that the calculated results differ substantially in a mean-field approximation.

The cavity is divided into two distinct space intervals, one related to the absorber section ($0 \leqslant x \leqslant L_{abs}$) and the other to the gain section ($L_{abs} < x \leqslant L$), where the injection rates per dot G_a and G_g are expressed in units of the inverse radiative lifetime $1/\tau_r$ (τ_r=1 ns). Figure 3 displays a schematic representation of the rate equation model.

The equations for the time and space dependent occupation functions $f_{GS}(t,x)=[N_{GS}(t,x)/2N_D]$ and $f_{ES}(t,x)=[N_{ES}(t,x)/4N_D]$, for the photon numbers per QD $n_{\varphi\pm}(t,x)=[N_{\varphi\pm}(t,x)/N_D]$ and for the WL population per QD $n_{WL}(t,x)=[N_{WL}(t,x)/N_D]$ can be summarized as follows:

$$\frac{\partial n_{WL}}{\partial t} = G_a - \frac{n_{WL}}{\tau_b} - \frac{n_{WL}(1-f_{ES})}{\tau_c} + \frac{4f_{ES}}{\tau_{esc}^{ES}}, \quad \text{if } 0 \leqslant x \leqslant L_{abs}$$

$$\frac{\partial n_{\mathrm{WL}}}{\partial t} = G_g - \frac{n_{\mathrm{WL}}}{\tau_b} - \frac{n_{\mathrm{WL}}(1-f_{\mathrm{ES}})}{\tau_c} + \frac{4f_{\mathrm{ES}}}{\tau_{\mathrm{esc}}^{\mathrm{ES}}}, \quad \text{if } L_{\mathrm{abs}} < x \leq L$$

$$\frac{\partial f_{\mathrm{ES}}}{\partial t} = -\frac{f_{\mathrm{ES}}}{\tau_r} - \frac{f_{\mathrm{ES}}}{\tau_{\mathrm{esc}}^{\mathrm{ES}}} + \frac{n_{\mathrm{WL}}(1-f_{\mathrm{ES}})}{4\tau_c} - \frac{f_{\mathrm{ES}}(1-f_{\mathrm{GS}})}{\tau_0} + \frac{f_{\mathrm{GS}}(1-f_{\mathrm{ES}})}{2\tau_{\mathrm{esc}}^{\mathrm{GS}}} - 8BN_D(n_{\varphi+}^{\mathrm{ES}} + n_{\varphi-}^{\mathrm{ES}})\left(f_{\mathrm{ES}} - \frac{1}{2}\right),$$

$$\frac{\partial f_{\mathrm{GS}}}{\partial t} = -\frac{f_{\mathrm{GS}}}{\tau_r} + \frac{2f_{\mathrm{ES}}(1-f_{\mathrm{GS}})}{\tau_0} - \frac{f_{\mathrm{GS}}(1-f_{\mathrm{ES}})}{\tau_{\mathrm{esc}}^{\mathrm{GS}}} - 4BN_D(n_{\varphi+}^{\mathrm{GS}} + n_{\varphi-}^{\mathrm{GS}})\left(f_{\mathrm{GS}} - \frac{1}{2}\right),$$

$$\frac{\partial n_{\varphi\pm}^{\mathrm{ES}}}{\partial t} \pm \frac{c}{n}\frac{\partial n_{\varphi\pm}^{\mathrm{ES}}}{\partial x} = 4\beta\frac{f_{\mathrm{ES}}}{\tau_r} - \frac{n_{\varphi\pm}^{\mathrm{ES}}}{\tau_\varphi} + 8BN_D(n_{\varphi+}^{\mathrm{ES}} + n_{\varphi-}^{\mathrm{ES}})\left(f_{\mathrm{ES}} - \frac{1}{2}\right),$$

$$\frac{\partial n_{\varphi\pm}^{\mathrm{GS}}}{\partial t} \pm \frac{c}{n}\frac{\partial n_{\varphi\pm}^{\mathrm{GS}}}{\partial x} = 2\beta\frac{f_{\mathrm{GS}}}{\tau_r} - \frac{n_{\varphi\pm}^{\mathrm{GS}}}{\tau_\varphi} + 4BN_D(n_{\varphi+}^{\mathrm{GS}} + n_{\varphi-}^{\mathrm{GS}})\left(f_{\mathrm{GS}} - \frac{1}{2}\right),$$

where a degeneracy 2 (4) was considered for the GS (ES) energy level, the radiative recombination is described by a lifetime $\tau_r = 1$ ns identical for GS and ES (determined by time resolved photoluminescence experiments), and a lifetime $\tau_b = 1$ ns is introduced for the WL population. The carrier exchange rate from one energy level to another always depends on a Pauli-blocking term of the form $(1-f)$, which prevents the carriers from being transferred when the final state is close to saturation. This term was neglected in the escape term from ES to WL, as the degeneracy of the WL is much higher than the one of the bounded states of the dot.

The escape times are derived by assuming that the system reaches quasi-Fermi equilibrium in the absence of external excitation,

$$\tau_{\mathrm{esc}}^{\mathrm{GS}} = \frac{\tau_0}{2}\exp\left(\frac{E_{\mathrm{ES}} - E_{\mathrm{GS}}}{k_B T}\right), \quad \tau_{\mathrm{esc}}^{\mathrm{ES}} = 4\tau_c \exp\left(\frac{E_{\mathrm{WL}} - E_{\mathrm{ES}}}{k_B T}\right),$$

where $E_{\mathrm{GS}} = 0.96$ eV, $E_{\mathrm{ES}} = 1.04$ eV, and $E_{\mathrm{WL}} = 1.14$ eV are the respective transition energies determined by high excitation photoluminescence experiments.

In the photon equations, β is the spontaneous emission coupling factor, characterizing the fraction of spontaneously emitted photons that go into the laser mode, and the photon lifetime can be expressed as $\tau_\varphi = n/c\alpha_i$, with the internal losses $\alpha_i = 3.5\ \mathrm{cm}^{-1}$, and where n is the waveguide effective refractive index. The mirror losses are taken into account as boundary conditions for the spatial dependent photon equations at the facet position ($x=0$ and $x=L$),

$$n_{\varphi-}(L) = R_2 n_{\varphi+}(L), \quad n_{\varphi+}(0) = R_1 n_{\varphi-}(0),$$

where R_1 and R_2 are the facet reflectivities.

The Einstein factor can be theoretically determined as

$$B = \frac{\lambda^4}{n^3 V 8\pi\tau_r \Delta\lambda},$$

with the laser mode wavelength λ, the gain spectral linewidth $\Delta\lambda$, and the optical mode volume V. To reproduce the experimentally determined value of GS saturated gain, this value was multiplied by a factor of 0.335. This reduced gain value may be related to nonradiative exciton states due to thermal spreading of holes in closely spaced valence-band states.[13] The interlevel relaxation time τ_0 was fixed to 7 ps as previously determined from fitting of *LI* characteristics of single-section lasers.[6,7] This is close to values determined by other techniques[14–16] and predicted by theory.[17] The capture time τ_c, whose value was checked not to play an important role, was fixed to 10 ps. This is also in the range of capture times reported by other authors.[18,19]

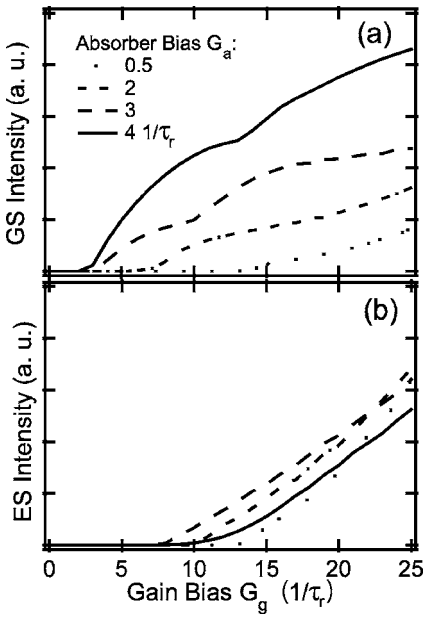

FIG. 4. Calculated GS (a) and ES (b) photon numbers vs carrier injection G_g in a QD two-section laser with a 2 mm long gain section and a 0.6 mm long absorber section at different bias levels G_a on the absorber section.

Figure 4 shows the calculated GS (a) and ES (b) photon numbers of a two-section laser with a 2 mm long gain section and a 0.6 mm long absorber section, corresponding to the experimental results in Figs. 2(a) and 2(b). In general, a very good agreement between experiment and simulations was found. Between absorber bias levels $G_a = 0.5-3\ 1/\tau_r$, a strongly decreasing GS threshold and a smaller amount of decrease on the corresponding ES threshold are observed, similar to the experiment. At $G_a 3/\tau_r$ GS threshold currents have reached their minimum value. In contrast to the experiment, however, ES threshold currents increase in this regime. In the model this increase stems from the fact that ES population in the gain section slightly decreases with absorber current due to the decreasing GS threshold population with a decreasing absorber loss. This discrepancy between experiment and model may be related to our simplified assumption of carrier density-independent interlevel relaxation times.

III. DYNAMICS

Time-dependent calculations in the model of GS/ES photon numbers reveal another behavior that is strongly connected to the two-state lasing mechanism. Figure 5 shows the time-dependent photon numbers of GS emission (a) and ES emission (b) of a two-section laser with a 2 mm long gain

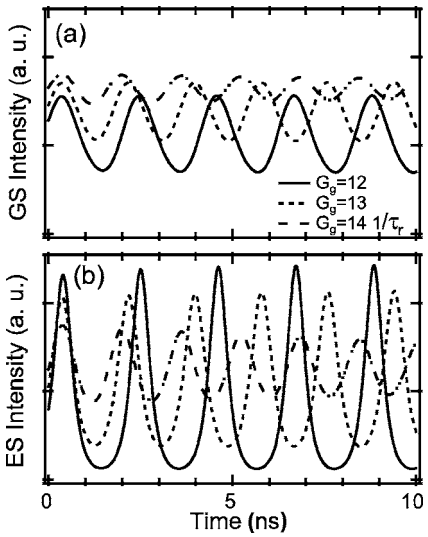

FIG. 5. Calculated dynamics of photon numbers on the GS transition (a) and on the ES transition (b) at various carrier injection rates G_g on the gain section and constant bias on the absorber section $G_a=3\tau_r^{-1}$ in a QD two-section laser with a 2 mm long gain section and a 0.5 mm long absorber section.

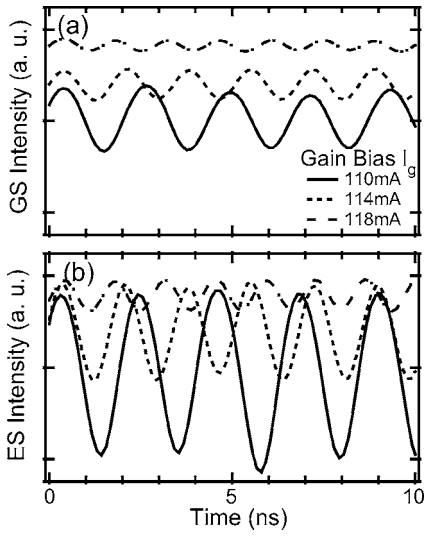

FIG. 6. Measured time-dependent GS (a) and ES (b) optical intensities at various injection currents I_g on the gain section and constant bias I_a =9.8 mA on the absorber section in a QD two-section laser with a 2 mm long gain section and a 0.5 mm long absorber section.

section and a 0.5 mm long absorber section for a constant carrier injection rate $G_a=3\tau_r^{-1}$ on the absorber section and different injection rates $G_g=12-14\tau_r^{-1}$ on the gain section, corresponding to the situation of combined GS and ES lasing. At the onset of ES lasing the occurrence of self-sustained pulsations is observed for both GS and ES photon numbers. The GS photon numbers at $G_g=12\tau_r^{-1}$ show a pulsation frequency of 0.5 GHz, which increases to a value of about 0.7 GHz at $G_g=14\tau_r^{-1}$. At the same time the pulsation amplitude decreases so that at injection rates $G_g>16\tau_r^{-1}$, the calculated GS photon numbers return to the steady state mode. The calculated ES photon numbers show a similar behavior, but the corresponding pulsation peaks are slightly narrower with larger amplitude. We note that GS and ES oscillations are synchronous, indicating that the respective populations are strongly coupled.

The modeling results have been checked experimentally on a two-section device with the same parameters assumed in the simulation. The temporal dependence of the filtered GS and ES intensities was measured with a fast (2 GHz bandwidth) digital oscilloscope in the free-running mode. The measured time-dependent output powers of GS and ES lasing are displayed in Figs. 6(a) and 6(b), respectively, with constant current injection in the absorber section (I_a =9.8 mA) and increasing current injection in the gain section (I_g=110–118 mA). We find exactly the same behavior as predicted by the model, with an onset of simultaneous GS and ES self-pulsations at the ES threshold, with amplitude decreasing with increasing gain bias, until a return to the steady-state mode at large gain bias. The self-pulsation frequency matches very well the theoretical result [which used the same parameters as the static calculations in Figs. 4(a) and 4(b)], while a slightly longer ES pulse duration is measured, probably due to the limited oscilloscope bandwidth.

While single-state self-pulsation in QD two-section lasers was observed previously,[20,21] the simultaneous GS and ES self-pulsations observed here is an intriguing consequence of the close interaction between the two states through interlevel carrier relaxation. Self-pulsation in two-section lasers is related to the positive feedback introduced by absorption bleaching in the relaxation oscillation dynamics. It occurs for large differential absorption and short carrier lifetime in the absorber, as compared to corresponding parameters in the gain region.[22] The former condition is easily obtained in QDs due to the strong saturation of gain under positive bias. In contrast, GS carrier lifetime is long in the absorber due to the strong electronic confinement. This explains why self-pulsation is obtained (both theoretically and experimentally) only in presence of ES lasing: rapid interlevel relaxation in the absorber produces a very short effective lifetime of the absorber ES. The strong coupling between ES and GS populations in the gain region then produces a coherent dynamics of both states. At even higher gain bias, the absorber bleaches due to higher photon number, which reduces the positive feedback and eventually suppresses the self-pulsation, as observed previously.[20]

IV. CONCLUSIONS

In conclusion, we have studied wavelength switching and the corresponding two-state lasing dynamics in QD two-section lasers. By varying carrier injection on the absorber section, the GS and ES threshold currents can be controlled. A complete switching between GS lasing and ES lasing could be observed with a reverse bias on the absorber. At ES lasing threshold the generation of simultaneous self-pulsating oscillations of both GS and ES intensities has been observed, as predicted by a traveling-wave rate equation model. These results show the potential for controlling the lasing state (and thus the wavelength) of QD lasers, and highlight the strongly coupled dynamics of the different QD states in lasing structures.

ACKNOWLEDGMENTS

We acknowledge the financial support from the Swiss NSF, EU FP6 project "ZODIAC" under Contract No. 17140, the Swiss CTI, and SER-COST programs.

[1]G. Park, O. B. Shchekin, D. L. Huffaker, and D. G. Deppe, IEEE Photonics Technol. Lett. **12**, 230 (2000).
[2]X. Huang, A. Stintz, C. P. Hains, G. T. Liu, J. Cheng, and K. J. Malloy, IEEE Photonics Technol. Lett. **12**, 227 (2000).
[3]O. B. Shchekin and D. G. Deppe, Appl. Phys. Lett. **80**, 3277 (2002).
[4]H. Saito, K. Nishi, A. Kamei, and S. Sugou, IEEE Photonics Technol. Lett. **12**, 1298 (2000).
[5]P. Bhattacharya and S. Ghosh, Appl. Phys. Lett. **80**, 3482 (2002).
[6]A. Markus, J. X. Chen, C. Paranthoën, C. Platz, O. Gauthier-Lafaye, and A. Fiore, Appl. Phys. Lett. **82**, 1818 (2003).
[7]A. Markus, J. X. Chen, O. Gauthier-Lafaye, J. G. Provost, C. Paranthoën, and A. Fiore, IEEE J. Sel. Top. Quantum Electron. **9**, 1308 (2003).
[8]A. Fiore, A. Markus, and M. Rossetti, Proc. SPIE **5840**, 464 (2005).
[9]B. Dagens *et al.*, Electron. Lett. **41**, 323 (2005).
[10]E. A. Viktorov, P. Mandel, Y. Tanguy, J. Houlihan, and G. Huyet, Appl. Phys. Lett. **87**, 053113 (2005).
[11]W.-D. Zhou, O. Quasaimeh, J. Philipps, S. Krishna, and P. Bhattacharya, Appl. Phys. Lett. **74**, 783 (1999).
[12]M. Rossetti, A. Markus, A. Fiore, L. Occhi, and C. Velez, IEEE Photonics Technol. Lett. **17**, 540 (2005).
[13]R. Heitz, A. Kalburge, Q. Xie, M. Grundmann, P. Chen, A. Hoffmann, and D. Bimberg, Phys. Rev. B **57**, 9050 (1998).
[14]T. Müller, F. F. Schrey, G. Strasser, and K. Unterrainer, Appl. Phys. Lett. **83**, 3572 (2003).
[15]M. De Giorgi *et al.*, Appl. Phys. Lett. **79**, 3968 (2001).
[16]T. F. Boggess, L. Zhang, D. G. Deppe, D. L. Huffaker, and C. Cao, Appl. Phys. Lett. **78**, 276 (2001).
[17]G. A. Narvaez, G. Bester, and A. Zunger, Phys. Rev. B **74**, 075403 (2006).
[18]J. Siegert, S. Marcinkevičius, and Q. X. Zhao, Phys. Rev. B **72**, 085316 (2005).
[19]T. S. Sosnowski, T. B. Norris, H. Jiang, J. Singh, K. Kamath, and P. Bhattacharya, Phys. Rev. B **57**, R9423 (1998).
[20]H. D. Summers, D. R. Matthews, P. M. Smowton, P. Rees, and M. Hopkinson, J. Appl. Phys. **95**, 1036 (2004).
[21]O. Qasaimeh, W.-D. Zhou, J. Phillips, S. Krishna, P. Battacharya, and M. Dutta, Appl. Phys. Lett. **74**, 1654 (1999).
[22]C. H. Henry, J. Appl. Phys. **51**, 3051 (1980).